Frontiers in Applied Physics, Materials Science and Nanotechnology
https://www.iahiservices.com

Research Article

Design and Construction of a Tensile Testing Machine for Laboratory Characterization of Shape Memory Alloys.

Abubakar Rabiu A[1*] https://orcid.org/0000-0001-8001-9788, Waqas Hafiz M[2] https://orcid.org/0009-0009-9251-4300, Gbaakpen Msughter[4] https://orcid.org/0009-0005-1756-013X

[1, 2,] Institute of Mechanical Design, Department of Mechanical Engineering, Zhejiang University, China
[3] Department of Science Laboratory Technology, Benue State Polytechnic, Ugbokolo
*Corresponding Author Email: rbkiru@yahoo.com

Abstract-The mechanical characterization of Shape Memory Alloys (SMAs) is critical for understanding their thermo-mechanical behavior and optimizing their performance in advanced engineering applications. However, the high cost of commercially available tensile testing machines with integrated thermal control limits accessibility, particularly in resource-constrained research and academic environments. This study presents the design and construction of a low-cost tensile testing machine tailored for laboratory characterization of SMAs, with emphasis on affordability, reproducibility, and educational utility. The system incorporates electromechanical actuation, microcontroller-based control, and thermal regulation to enable precise measurement of SMA properties under variable loading and temperature conditions. Comprehensive design documentation, fabrication details, calibration procedures, and testing protocols are provided to facilitate replication. The developed machine was validated through tensile tests on SMA springs, with experimental stress–strain curves showing strong agreement with numerical simulation results. Comparative analysis confirms the system's accuracy and operational stability, demonstrating its suitability for both research and instructional use. The proposed design offers a cost-effective alternative to commercial systems, thereby enhancing accessibility to advanced materials testing in low-resource settings.

Article Key Information

Keywords: Tensile Properties; Shape Memory Alloys; Digital Force Gauge; Thermo-Mechanical Coupling

Received:11th June 2025 **Revised:** 7th August 2025 **Accepted**: 8th August 2025 **Published**: 9th August 2025

1. Introduction

Shape Memory Alloys (SMAs) represent a class of advanced functional materials distinguished by their ability to recover a predetermined shape when subjected to appropriate thermal or mechanical stimuli. Among SMAs, Nickel–Titanium (NiTi) alloys are particularly notable due to their exceptional shape memory effect, superelasticity, biocompatibility, and corrosion resistance, making them suitable for a wide range of applications in biomedical devices, aerospace systems, robotics, and actuators [1–4]. The mechanical characterization of SMAs is essential for optimizing their performance in such applications, as their unique thermo-mechanical properties differ significantly from those of conventional engineering materials [5,6].

Tensile testing remains a fundamental approach for assessing the mechanical behavior of materials, providing critical data on stress–strain relationships, elastic modulus, tensile strength, and deformation characteristics [7]. For SMAs, tensile testing is particularly important for evaluating phase transformation behavior, hysteresis characteristics, and the effect of temperature on material performance [8]. However, commercially available tensile testing systems equipped with thermal control units and precision instrumentation are often prohibitively expensive, limiting their accessibility to institutions and laboratories with restricted budgets [9–11]. This constraint is especially significant in developing regions, where the high cost of equipment poses a barrier to research and education in advanced materials.

Several low-cost tensile testing systems have been reported in literature, incorporating custom-built fixtures, microcontroller-based control systems, and electromechanical actuation to provide affordable alternatives [12–15]. While these systems demonstrate varying degrees of success, many lack integrated thermal control for studying SMA behavior under realistic service conditions, and others compromise on measurement precision, repeatability, or load capacity. In academic settings, an ideal low-cost solution should not only meet accuracy requirements but also support experimental versatility, enabling both mechanical and thermo-mechanical characterization.

In response to these challenges, this study presents the design and construction of a low-cost tensile testing machine specifically tailored for SMAs, with emphasis on affordability, ease of fabrication, and educational utility. The system integrates electromechanical actuation, microcontroller-based control, and thermal regulation capability to enable precise laboratory testing of SMA springs and wires. Detailed documentation of the design process, assembly, calibration, and testing protocols is provided to facilitate reproducibility. The machine's performance is validated by comparing experimental stress–strain results with numerical simulations, thereby demonstrating both the accuracy and applicability of the developed system.

2. Materials and Methods

2.1 Conceptual Design

The machine is designed to have a single-column stand with a sliding bed attached to the upper part. A step motor is attached to the upper end of the sliding bed, controlling the movement of a cross-head along a screw-threaded shaft. There is a digital controller attached to an adjustable stand and a digital force gauge attached to the cross-head. There are three grippers with one attached to the loading cell, the second gripper attached at the middle of the column, and the third one attached to the base of the machine. A water heater holder is attached to the lower part of the column stand, and a cap covers the column and step motor from the top. The design of the machine is actualized as follows:

2.2 Components required to be designed and constructed

The machine consists of the following main parts:

i Frame

ii Moving head

iii Sliding bed actuator (model no. 1605). This consists of a step motor, screw rod, moving nut, and bearing

iv SMA wire gripper

v (ST-PMC1) single-axis motion controller

vi Digital force gauge (model no.: HP-500N)

vii Heating Chamber

The components to be designed and fabricated are the moving cross-head, frame, and heating chamber. The remaining components which include the loading cell, controller, Arduino, step-motor, and sliding bed are purchased from the store and assembled.

Design of the frame

The frame of tension testing equipment consists of 3 major parts which are given below and described separately. A few factors have been considered in designing the frame to increase operator safety, accuracy of results, and cost reduction. It is single-column vertical testing equipment a force sensor is installed on the moving crosshead to measure precisely while a control unit is installed on the side to make it safe for the operator and easily connect with power and computer. The main structure is made of steel to make it stable and support heavy objects and a hot water chamber for SMA spring testing.

The main components are given below:

i. Frame
ii. Moving crosshead
iii. Water heater chamber holder
iv. Elongation scale

Frame

The frame is single-column support. The main part of the frame is a table base on which the column stands. The base has a gripper where the specimen for the application of tensile test is attached. We have used a rectangular pipe with an outer size (80x60) mm and a thickness of 3mm for the frame body. The stress on the frame is calculated as:

$$\sigma = \frac{F}{A} \quad (1)$$

The effective area of the rectangular pipe is calculated as:

$$[(80 \times 60) - (74 \times 54)] \times 10^{-3} = 0.804\, m^2,$$

$$\sigma = \frac{150}{0.804} = 186.6 \approx 200\, Nm^{-2}.$$

Using the factor of safety of 2.5, the stress is going to be *500 N/m²* on the frame.

The moving crosshead

Figure 1 shows the engineering drawing of the crosshead. It is the component that carries the force sensor and is attached to the moving nut of the sliding bed. The upper crosshead is used to test the specimen. The lower crosshead is the part that is movable, and its screws may be loosened for adjusting the height of the crosshead. Both of the crossheads are marked with a tapered slot at the center. These slots have racked jaws pairs which are mainly used for holding and gripping the specimen during the tensile test. The moving crosshead was constructed using mild steel and it is shown below:
Hence, from Figure 1,

$$\sum f_{x=0}; \quad \sum f_{y=0}; \quad \sum M_{A=0}$$

$$F_y = 150$$

$$F_x = 0$$

$$MA = 75\, x\, 150 x\, 10^{-3} = 11.25\, Nm$$

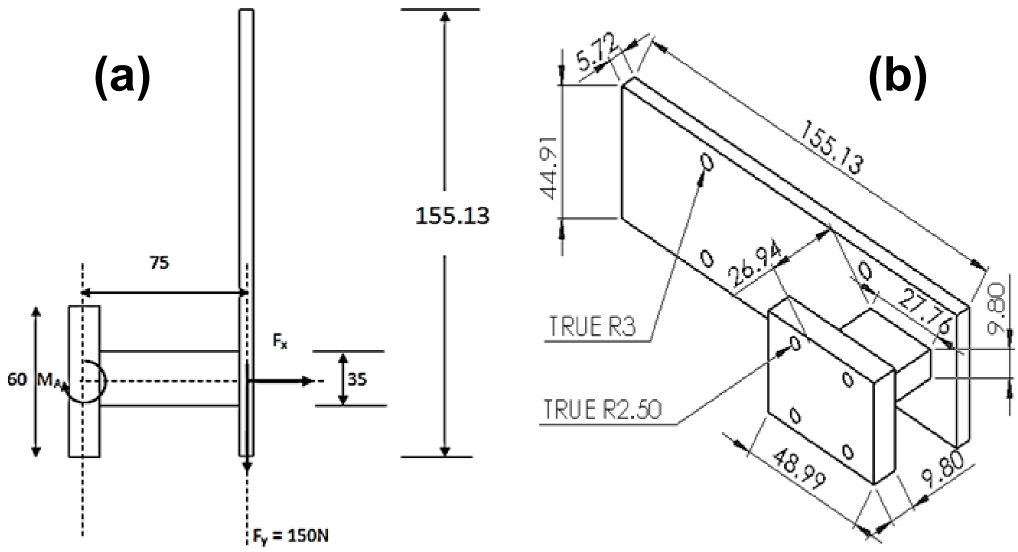

Figure 1: (a) Moving cross Head 1, and (b) Moving crosshead 2

Elongation scale

The elongation scale is the part that is generally used for measuring the length of the cross-head. It is placed on the frame and has a total length of 1000mm.

Digital Force Gauge

It has various testing modes, convenient to store data in the device and transfer it to computer for statistical analysis as well as constitutes testers with different functions, in combination with test-beds and clamp. A step motor is attached at the top of the device to rotate the spindle. The force sensor is attached with a spindle which is rotated by the top-mounted step motor. This force sensor is limited to measuring up to 150N, and it will be connected to a computer to get the experimental data.

Feature:

i. Five testing modes and three display methods are available to enhance testing efficiency to the maximum extent.

ii. Three measuring units N (Newton), kg (Kilogram), and, lb. (Pound) for selection and conversion.

iii. Maintain the display result of peak value until manually cleared.

iv. Max and min comparison values can be set for statistical analysis. The buzzer will alarm if exceeding the comparison value.

v. Up to 896 testing results can be stored for later use.

vi. The data can be transferred through a cable to a computer for analysis.

The following modes are associated with the loading cell:

i. **PEAK**

When "PEAK" is displayed, it indicates Peak mode (Peak maintaining mode), it will keep displaying the peak value until manually cleared. If "AUTO PEAK" is displaying, it means Automatic release mode of peak maintenance and the display of peak value will be maintained for 2 seconds and then cleared automatically. When "PEAK" is not displayed, it tells "track mode" (Real-time load value mode), and the value will change on the screen according to the applied load.

ii. **LO BAT**

If the voltage is below 7.0V, the screen displays "LO BAT", which means the batter is low (Testing can be carried out during charging)

iii. **MEM**

When the data is saved in the storage, "MEM" will be displayed. When the "DATA" button is pressed to check memorized data, "MEM" will flash.

iv. **Display**

In this mode, default thrust (tension) is the negative value（“-”), pull value is the positive value （“+” not displayed)

v. **CMP Comparative function.**

When adjusting comparative value through CPDT, this function will be activated and display "CMP". Comparative default is considered as the complete measuring range, it can be changed according to demand.

vi. **SET Button functional setting**

Figure 2 shows the setting buttons. When the device is powered on, press the SET button. The items to be set will be displayed. The first displayed option is "TEST", a digit setting window will appear after 2 seconds. Set the testing mode by using the SEND button and SET button. Then press the SET button, and "AODT", "LODT", "HIDT" and "CPDT" will appear in turn. The digit setting window will be displayed automatically at the corresponding item after 2 seconds.

Set the desired parameters by pressing the SEND button and the MEMO button. "Set end" will be displayed, which indicates the setting is finished and enter testing status. TEST is expressed by four digits with the following definitions; 0000 real-time load value mode. 0001 standard testing mode; 0002 push-pull peak value mode; 0003 pull peak value mode; 0004 push peak value mode; 0005 external contact break-make mode; 0006 external contacts make-break mode; 0000 real-time load value (Random tracking) mode. Under any status, keep track of changes in the display of testing data value. When the testing data value disappears and returns to the zero point. At the time, PEAK couldn’t play its function. **0001 standard testing mode** (Default mode) three kinds of status can be set, real-time load value status, peak value maintaining status, and automatic peak value status. When there is no "PEAK" on the screen, it is under real-time load value status. The testing value will change accordingly with a load. Press the Peak button, and "PEAK" will be displayed on the screen which will be peak maintaining status. The displayed testing value is the maximum value in the test (pull force or pressure). Press the PEAK button again, and "AUTO PEAK" is going to be displayed on the screen, which is the indication the device is in automatic peak status. The displayed testing value is the maximum value in the test (pull force or pressure), this value will disappear after 2 seconds of the display.

0002 push-pull peak value mode measures the function of maximum load value at the two directions of pressure and pull force. In connector testing it measures the function of maximum load value (Fc, Ft) of positive and negative directions of push and pull force.

0003 pull peak value mode during push-pull testing, only controls the function of maximum load (Ft) of pull force.

0004 push peak value mode during push-pull testing, just measure the function of maximum load (Fc) of push force.

0005 and 0006 switch contact make-break testing mode Measure the accurate load value during the instant action of making and breaking of contact.

When the added load is larger than the setting value of Fa, until the contact changes from breaking to making or from making to breaking, the load value on the screen will stop its change, the value displayed is the tested value.

Connect PIN 4 and PIN 5 of the data interface as the contact signal (Through the data plug in the accessories).

If F_a is not set (Sensing range), the testing can’t be carried out.

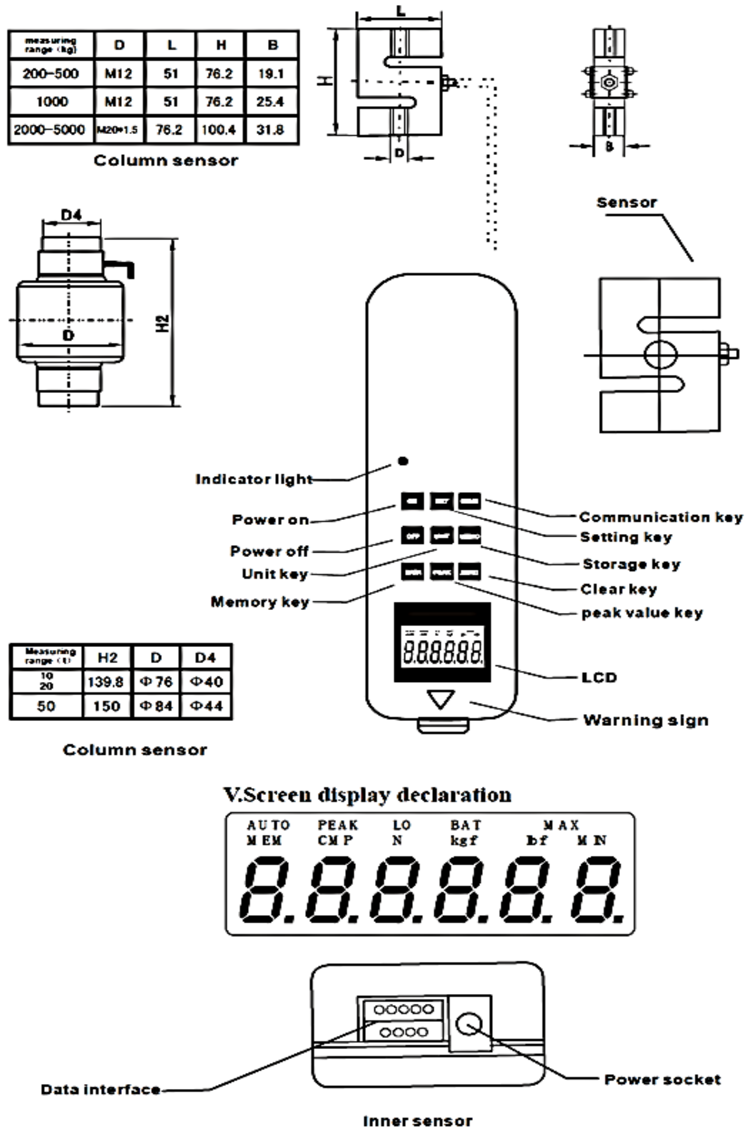

Figure 2: Structural diagram of a force sensor.

AODT Setting of sensing value

Set the sensing value F_a to test both the pull and push function at the same time. For example:

In push force testing, if the value exceeds the sensing value, it indicates "Push" to start the testing, and then, the value will be lower than the sensing value, which indicates the push force testing is finished. On the other hand, the pull-force testing in the reverse direction can be carried out. If the value exceeds the sensing value, it indicates "Pull" starts the testing, and then, the value will be lower than the sensing value, which indicates the pull force testing is finished.

LODT Setting of Min

Set the Min of testing value, if a value is lower than Min, the value will exceed the range, and "MIN" will be displayed.

HIDT Setting of Max

Set the Max of the testing value, if a value is higher than the Max, the value will exceed the range, and "MAX" will be displayed.

CPDT Setting of comparison value

When the testing value exceeds the set comparison value, the buzzer will alarm. LODT, HIDT, and CPDT are used together to make the apparatus analyze and judge the ability of testing data. When a user is not clear about the debugging, (it's better to return to power on status after power off), press the setting button for more than 4 seconds, leave your hands until hearing the "DI" sound, and the apparatus can return to the default value status. The values are shown as follows:

TEST: 0001 in standard testing mode; AODT, LODT: 1% of complete measurement range

HIDT, CPDT: full measurement range.

Data interface (9PIN)

There are 9 pins at the back of the force sensor as shown in Figure 3; each pin has a different function which is shown in Figure 3.

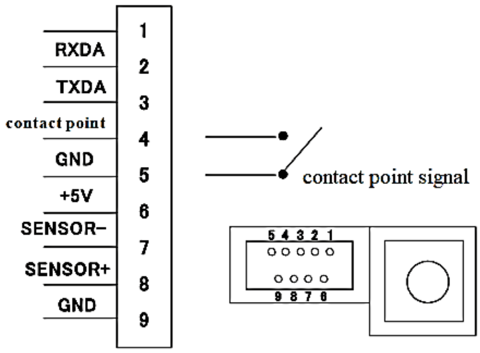

PIN	FUNCTION
PIN4 PIN5	Contact point signal
PIN2 PIN7 PIN8 PIN9	Structure names and graph
PIN2 PIN3 PIN9	RS 232 interface to computer

Figure 3: Outline and mounting dimension chart.

Control Unit

Load exertion or the test specimen arrangement is held mostly in the loading unit. Corresponding test variations and the load application are usually obtained from the unit known as the **control unit**. It further categories into two main parts.

1). Load Measuring Unit

2). Control Devices

Load Measuring Unit

Figure 4 shows the single-axis step-motor operation panel. The grips deflect the specimen which is based on the load that is applied on the specimen. The applied deflections are converted into the load pointer, which is then displayed as the load and can be seen on the control unit display.

Application load range can be adjusted within the unit of load measuring range, usually marked with the units 0 - 1000 KN, 0 - 500 KN, 0 - 250 KN, and 0 - 100 KN). The overall accuracy of a machine is determined by the accuracy of the measuring unit.

We have used the electrical control unit which consists of switches and buttons the reason to use an electric control system is due to its precision. It is easy to operate buttons that will be used to relocate or input the data it also has a digital meter that shows input commands and the results. It is attached to the side of the tension tester and connects with the step motor to control its speed and position.

Features

i. Single axis which can achieve a variety of complex operations: positioning control and non-positioning control.

ii. The maximum output frequency: is 40 kHz.

iii. Output frequency resolution: 1Hz.

iv. Programmable maximum number of rows: 99.

v. A continuous displacement range: -7,999,999 ~ 7,999,999.

vi. Operating state: Auto-run mode, manual operation, the program edit mode, parameter setting status.

vii. Auto-run feature: You can edit and control the start and stop operation through the panel buttons by adding switches that connect to the back of the terminals.

viii. Manual operation functions: position adjustment (manual jog speed and jog the number of steps can be set).

ix. Parameter setting function: Starting frequency, acceleration and deceleration curve, reverse clearance, manual run length, manual speed, back to zero speed, and interrupt jump the line can be set.

x. Program editing functions: You can insert, delete, and modify the program. The controller can identify the error Instruction.

xi. Return to Zero features: It can return to zero from the positive and negative directions.

xii. External operating functions: interrupt operation through parameter setting and add switches that are connected to terminals A and B.

xiii. Power supply: DC 24V.

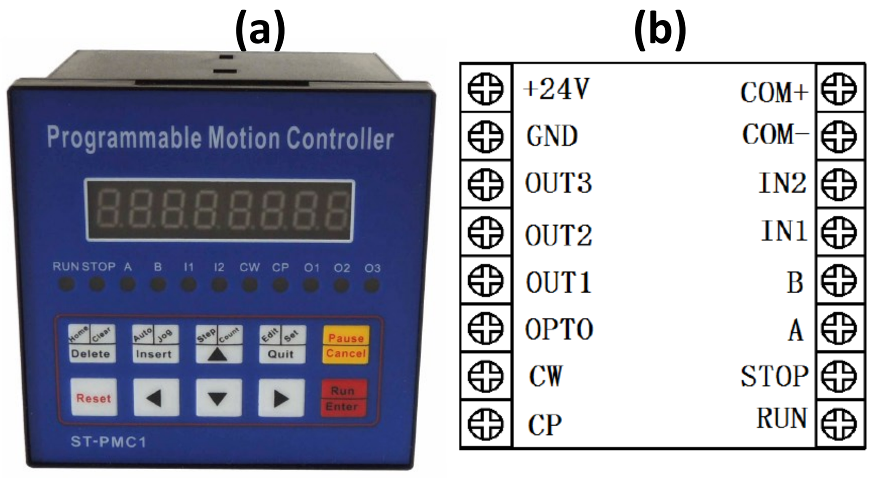

Figure 4. Labeled Components of the Tensile Testing Machine Control Panel (a) Single-axis step-motor operation panel (b) Back panel diagram.

Figure 4 shows the labeled components of the tensile testing machine control panel which are listed below:

1. Eight-digit LED segment display.
2. Six input status indicators.

3. Output status indicator.
4. CP (Clock Pulse) signal indicator.
5. CW (Clockwise) direction signal indicator.

Back panel diagram and signal descriptions

1). **CP, CW, OPTO** for stepper motor drive signal.

2). **CP:** pulse signal.

3). **CW:** direction signal.

4). **0PT0:** Public male end before the two signals.

5). **RUN:** Start running the program, The same function as "**Run**" of the operation panel.

6). **STOP:** It is the same function as "**Pause**" of the operation panel, after starting again, the program continues to run.

7). **A:** An operation; **B:** B operation.

"An operation" and "B operation" this is a major feature of the controller. For stepper motors, we generally use quantitative positioning control, such as controlling the displacement of the motor must be running at a constant speed. It is easy to control by just inserting the amount and speed of displacement in the program.

1). **IN1** and **IN2** Switching signal input terminal.

2). **OUT1**, **OUT2,** and **OUT3** Switching signal output terminal.

3). **COM +**, **COM-**: the power supply of external input and output devices, this power supply is DC24V, **COM +** is the positive terminal of the power supply, **COM-** negative side.

4). **+24V:** The positive power supply, **GND:** Negative power supply.

The signals **RUN**, **STOP**, **A**, **B**, **IN1**, and **IN2 are** called the input signal, they have the same input interface circuit. **OUT1**, **OUT2**,**0UT3** called the output signal. They have the same output interface circuit. Both input and output optical isolation circuits to ensure that the internal and external controllers do not interfere with each other; The state of the input signal and output signal of the corresponding indicator will be displayed on the panel. When the input is low the switch will be closed and the Indicator light will turn on. For the output signal, when output 0 is low, the light will remain off. Figure 5 shows (a) Input circuit switch and (b) Output circuit switch.

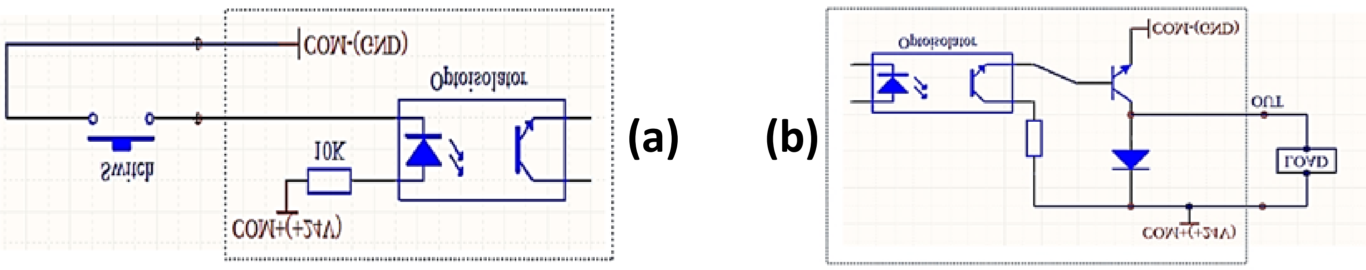

Figure 5: (a) Input circuit switch (b) Output circuit switch.

When the switch is turned on, the input level is low, the front panel indicator lights turn ON, and the program is defined as 0.

In case of low output or load conduction, the front panel indicator lights turn ON, and the program is defined as 1.

The controller connection diagram

The controller connection following the diagram is shown in Figure 6.

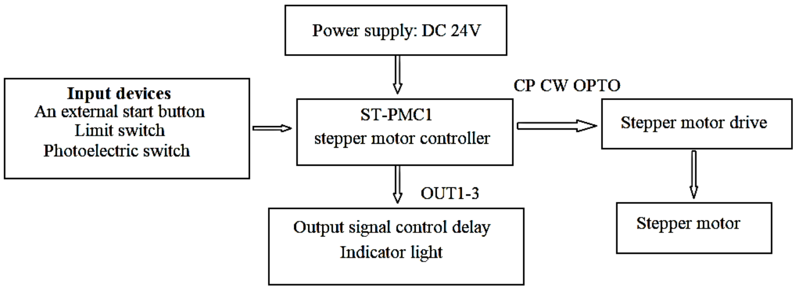

Figure 6: Controller connection diagram.

Operation flow chart

Figure 7 shows the controller flow chart. It always operates in one of four states: automatic mode, manual mode, the program edit mode, and parameter setting state. Power or press the **Reset**, Controller to run in automatic mode, the cursor coordinates 0, then you can start the program to run automatically or switch to manual mode, program editing state and parameter setting status can only switch in manual mode. When the editing or the parameter setting procedure is completed, press the **Quit** to return to manual mode (the program will be saved), in manual mode, if you switch to program edit mode, simply press the **Edit** button, if you switch to the parameter setting state, press and hold **Set** button for more than 2 seconds.

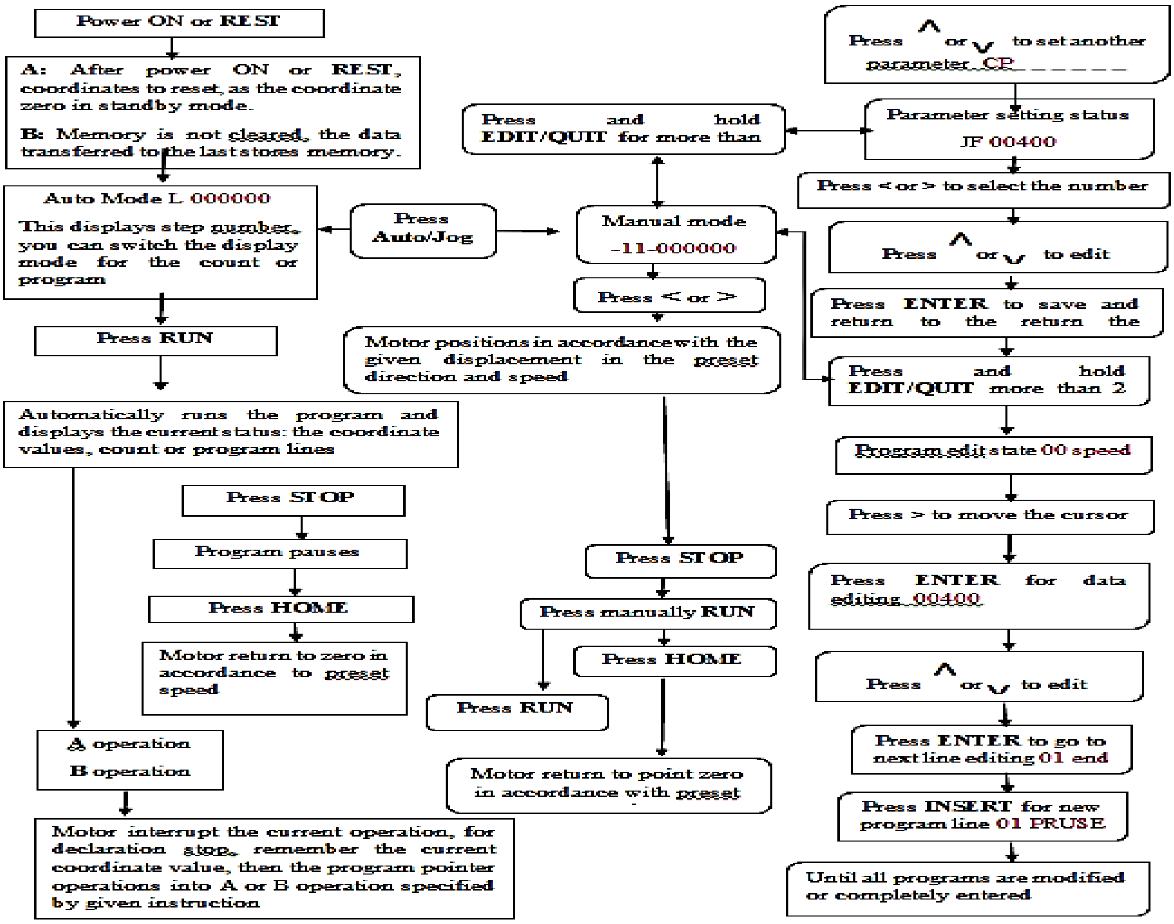

Figure 7: Flow chart of controller.

2.2. Design Drawing

Figure 8 shows the Autographic view of the SMA tensile testing machine. The model has been designed in Solidworks, and the Autographic view is presented here. The figure clearly presents the force tester and the loading plane, which will load the SMA spring and the force stretch will be noted, which will act as the experimental data.

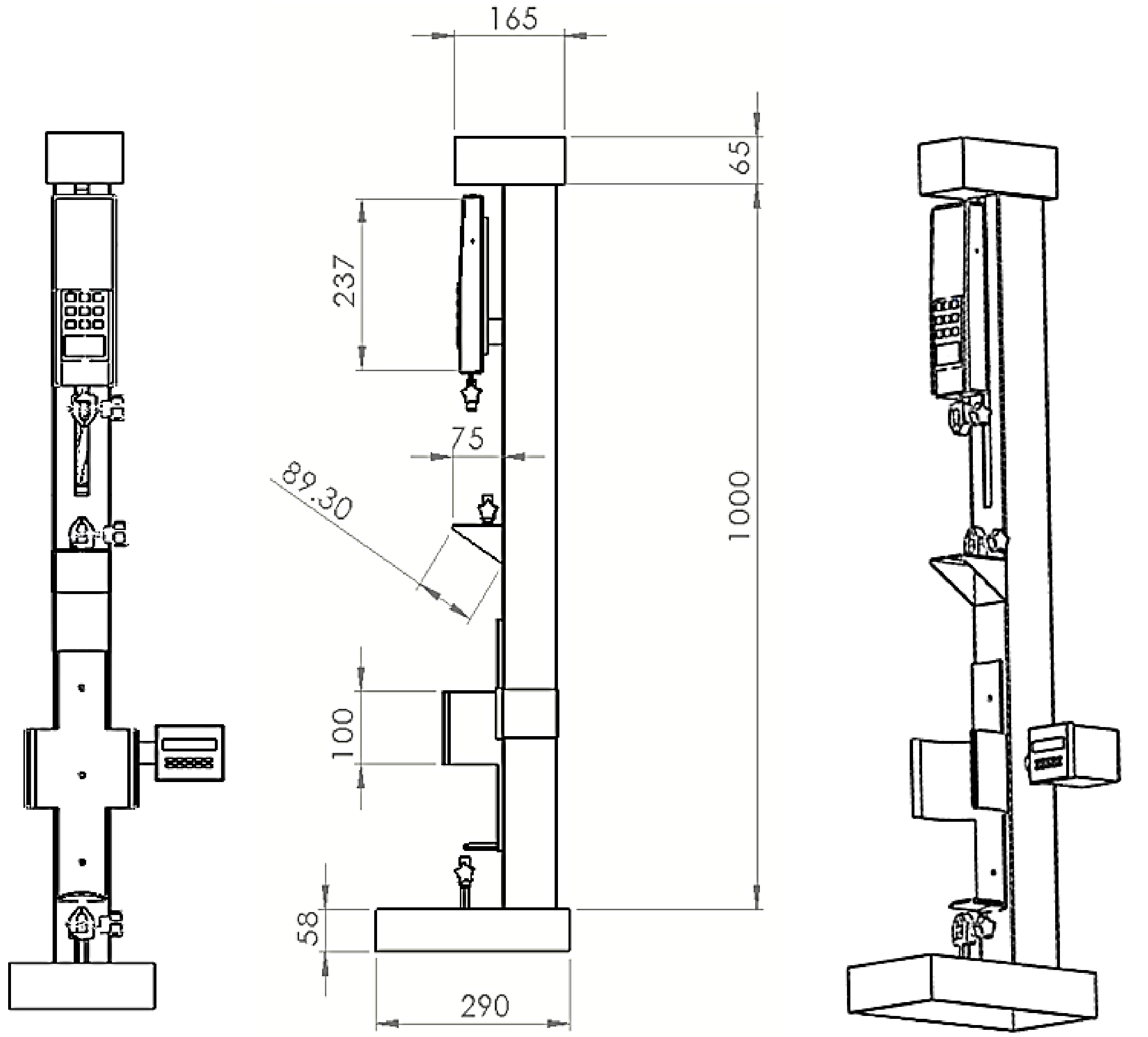

Figure 8: Autographic view of The SMA machine.

2.3. Assembly of components

A detailed view and assembled view of the SMA tension testing equipment is presented along with its exploded view. The red box on top is used to cover the stepper motor and placed on the top of the load cell in Figure 9. The stepper motor is located right under the top case which is connected to a spindle and helps it to rotate, the force sensor is also mounted on the moving head which is attached to the spindle, and it moves by spindle movement. There is a gripper attached under the forced sensor which is used to hold the testing object. The gripper in the middle is attached to use the device at room temperature without a heating chamber. There is a semi-circled holder for the heating chamber, and the gripper is also placed just below the heating chamber to hold the object during the temperature-controlled experiment. An electrical control unit is also displayed on the right side of the device, which is mainly used for controlling the stepper motor.

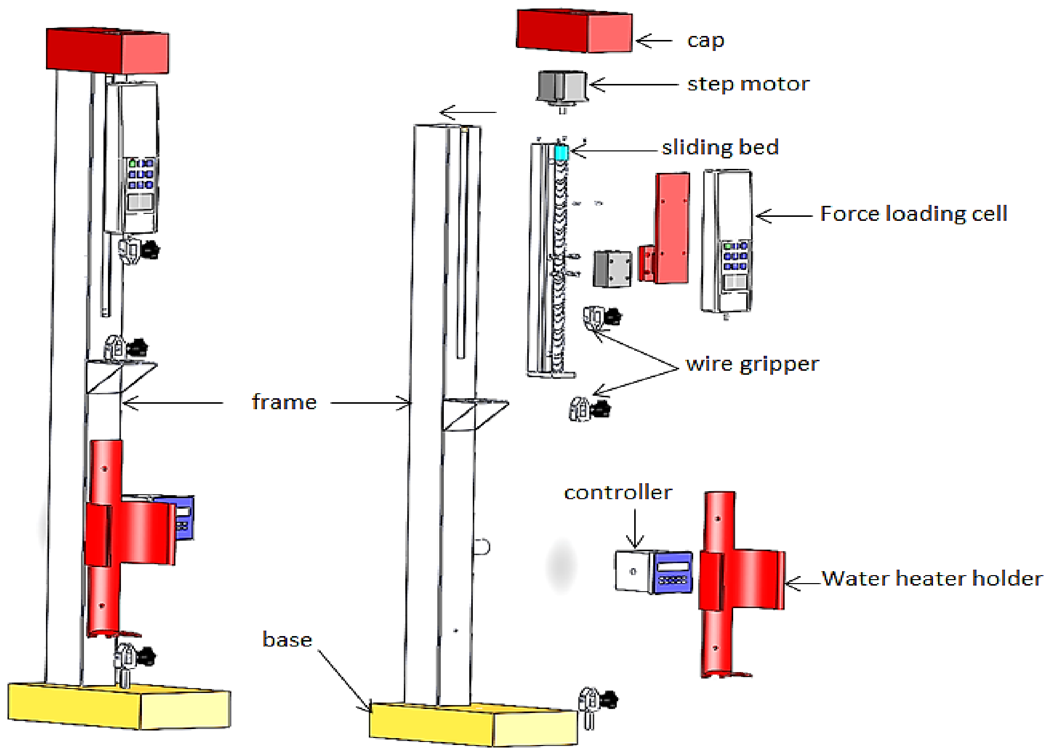

Figure 9: SMA Spring tension test machine (left), Exploded View (right).

2.4. Estimated Cost Analysis

The detailed cost analysis for constructing the tensile testing machine for Shape Memory Alloy (SMA) laboratory tests is presented in Table 1. The total expenditure amounts to 905 Yuan (approximately 125 USD), which includes structural, mechanical, and sensor components as well as labor.

Table 1. Cost Analysis

No.	Component	Material	Quantity	Property	Price (Yuan)
1	Frame	Steel rectangular pipe (80×60)	1	500 N/m²	100
2	Sliding bed actuator	—	1	1605	332
3	Wire gripper	Steel	1	—	62
4	Force sensor	—	1	50 kg	500
5	Connecting wire	Copper	1 m	0.3 mm	25
6	Labour	—	—	—	150
	Total				**905**

To contextualize this cost**,** commercial tensile testing machines suitable for SMA testing typically range between 20,000–50,000 USD**,** depending on features such as extensometer integration, load cell precision, and automated control systems. Even low-cost academic prototypes, as documented in recent literature, average 1,000–3,000 USD in material and labor expenses [26], [27].
Given this, our design—completed for under 130 USD—offers a **cost** reduction of over 90**%** compared to commercial alternatives and significantly undercuts academic builds**,** without sacrificing core functionality such as load measurement, displacement control, or extensometer compatibility. This makes the proposed machine highly accessible for resource-constrained laboratories, especially in developing regions or educational settings.

2.5 Construction

The construction process involves only the two components. The remaining components are selected from a store and assembled. In the first place, the frame is constructed from a rectangular hollow pipe made of steel, followed by the construction of the crosshead. The construction involves cutting the parts to the designed size, followed by welding using electric arc welding. Figure 10 shows the engineering drawing of the frame and cross-head fabrication.

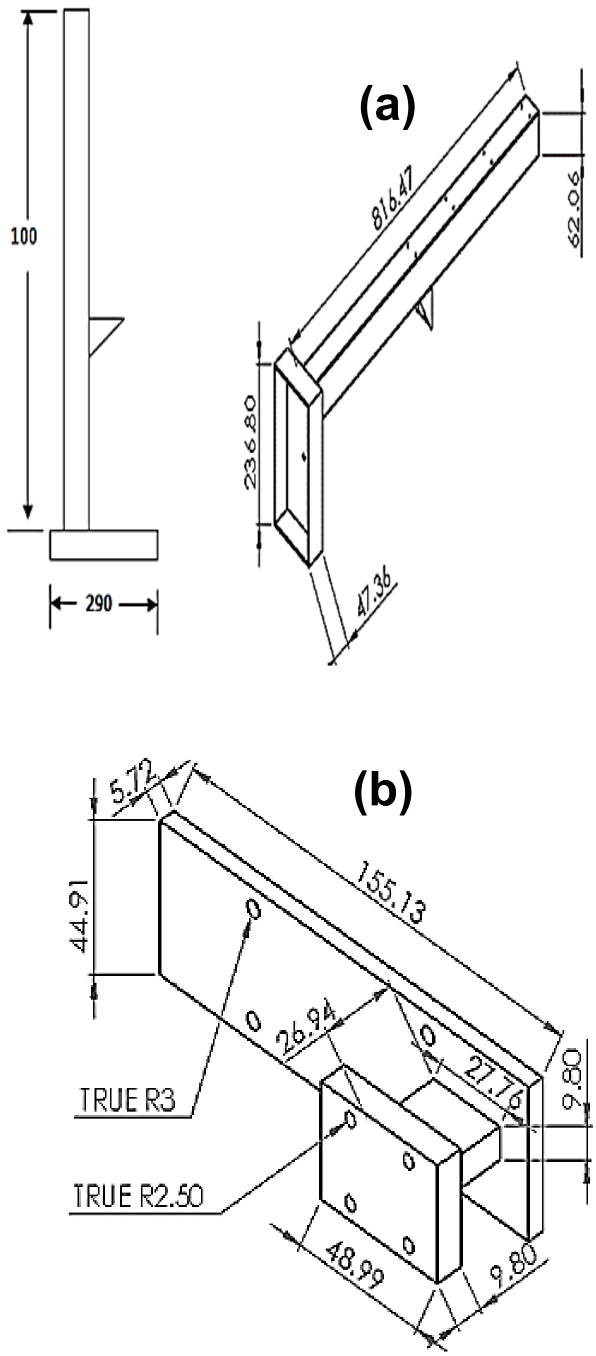

Figure 10: Frame and cross-head fabrication.

2.6. Experiment Test

Figure 11 shows the experimental setups. The experimental procedures were conducted using a custom-built tensile testing machine specifically designed for Shape Memory Alloy (SMA) materials. The methodology was structured to ensure precision, repeatability, and reproducibility. The key stages of the experiment are as follows:

2.6.1 Specimen Preparation

Nickel-titanium (NiTi) shape memory alloy wires with a diameter of 1.0 mm and a gauge length of 50 mm were used. Each specimen was cut to size using a precision wire cutter, and both ends were attached to a specially designed bolt and nut which is welded to a steel wire, and then securely in the grips of the testing machine to avoid slippage or misalignment during loading.

2.6.2 Strain Measurement

The strain was measured using a clip-on extensometer with a gauge length of 25 mm, providing a direct measurement of axial strain on the SMA specimen. The extensometer was calibrated prior to use and conformed to ASTM E83 Class B-1 accuracy requirements. In parallel, crosshead displacement was also recorded through the machine's integrated linear encoder (resolution: 0.01 mm), and this data was used only as a secondary measure to validate extensometer readings.

2.6.3 Force Measurement and Sensor Calibration

Force was measured using a load cell with a 500 **N** capacity, integrated into the machine's frame. The load cell was calibrated using a traceable deadweight calibration procedure, following ISO 376 standards. A series of certified weights were applied incrementally, and the sensor's response was recorded and used to generate a calibration curve, with linearity confirmed up to 0.995 R^2.

2.6.4 Test Procedure

Each tensile test was performed at room temperature (22 ± 1 °C) and under displacement-controlled loading at a constant rate of 1 mm/min to ensure uniform strain rate. The test continued until a defined elongation limit was reached or the specimen failed. All data (force, displacement, strain) were collected at a sampling rate of 10 Hz via a DAQ system and logged for analysis.

2.6.5 Repeatability and Reproducibility

To assess the reliability and repeatability**,** each experiment was repeated five times for each SMA specimen configuration. The data were analyzed statistically, and standard deviation and coefficient of variation (CV) were computed for peak stress and strain to quantify variability. Between tests, the machine was reset and zeroed, and the extensometer was removed and reattached to ensure consistency across runs.

2.6.6 Safety and Error Management

The alignment of the specimen was visually confirmed before each test. Any specimen exhibiting signs of torsion or off-axis loading was discarded. All sensors and electronics were grounded and shielded to minimize noise during data acquisition.

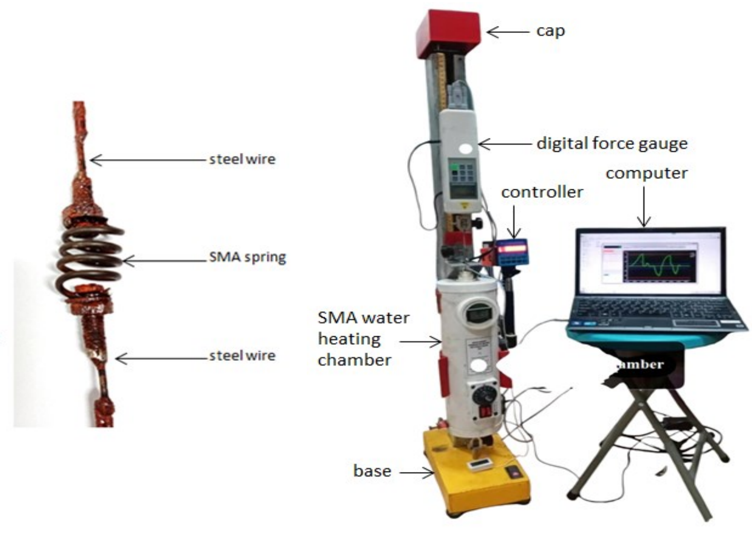

Figure 11: Experimental setups.

3. Results and Discussion

3.1. Results

The experimental and simulation results for SMA springs under tensile loading are presented in Figure 12. The goal of this comparison is to evaluate the ability of the fabricated testing machine to replicate known thermo-mechanical behaviors of Shape Memory Alloys, particularly the characteristic hysteresis observed during loading and unloading.

Springs of varying lengths (50 mm, 60 mm, 70 mm, 80 mm, 90 mm, and 100 mm) were tested under a constant temperature of 50°C and a fixed loading rate of 0.5 mm/s. For each spring, the force-stretch behavior was recorded and then compared to simulations based on a standard constitutive model for SMAs.

Figure 12(a–f) presents the simulation and experimental data for each spring length. In all cases, the results show a clear hysteresis loop, typical of SMA behavior, with a strong alignment between the experimental and simulated curves. The experimental data closely track the simulation predictions, particularly in the loading segments. Minor discrepancies are visible during unloading, especially at higher strains, which may be attributed to friction, sensor lag, or material inconsistencies.

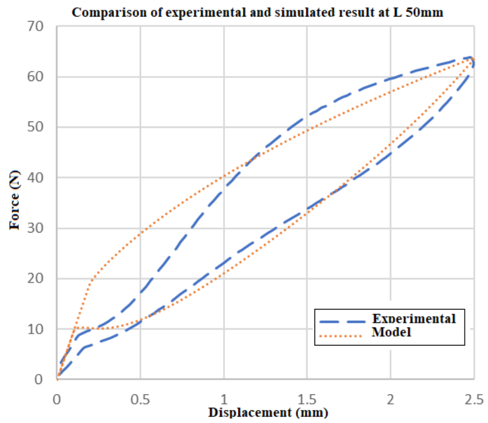

(a) *L* 50mm at *T* 50 °C and loading rate 0.5mm

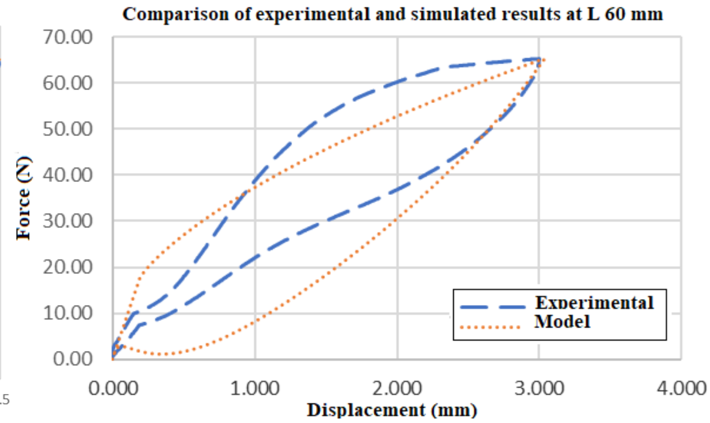

(b) *L* 50mm at *T* 60 °C and loading rate 0.5mm

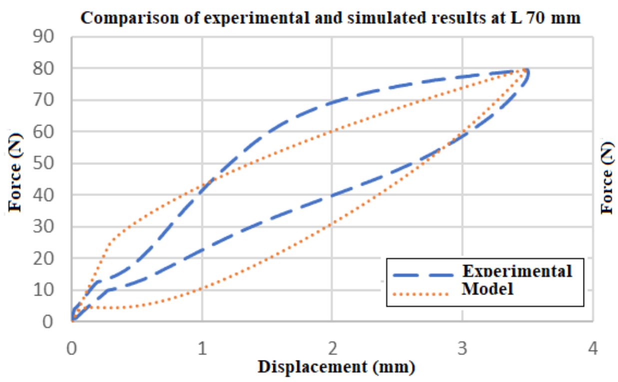

(c) *L* 70mm, *T* 50 °C, and loading rate 0.5mm/s.

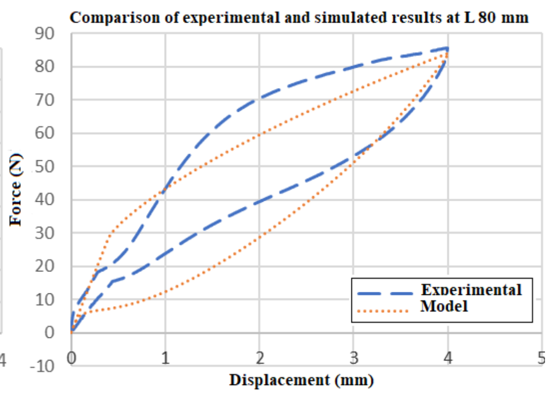

(d) *L* 80mm *T* 50 °C and loading rate 0.5mm/s

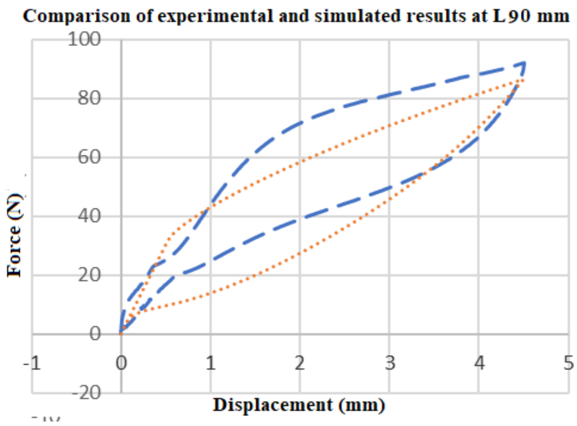

(e) *L* 90mm, *T* 50 ºC and loading rate 0.5mm/s

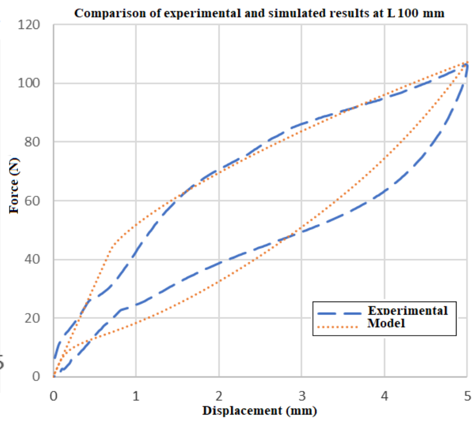

(f) *L* 100mm *T* 50 ºC and loading rate 0.5mm/s

Figure 12: Comparison of experimental and simulated results of SMA Spring.

3.2. Discussion

The comparison between experimental and simulated data validates the performance of the constructed tensile testing machine. The close match in force–stretch curves indicates that:

- **Accuracy**: The device captures the nonlinear and hysteretic response of SMAs with reasonable fidelity. The alignment between experimental and simulated results demonstrates that both force and displacement measurements are reliable.
- **Sensitivity**: The device is sensitive enough to detect the onset of phase transformation, evident from the inflection points in the force-displacement curves.
- **Reproducibility**: Similar curve shapes and trends were obtained across multiple spring lengths, suggesting consistent performance.
- **Limitations**: Slight deviations in unloading behavior could arise from several sources:
    - Minor backlash or compliance in the mechanical components (e.g., wire gripper or actuator).
    - Possible temperature gradients, despite nominal control.
    - Lack of strain-specific instrumentation such as extensometers or digital image correlation (DIC), which could improve precision.

Importantly, no formal error analysis or uncertainty quantification was included in the current work. This limits the statistical confidence in the results. Future experiments should:

- Include multiple repeated trials to assess repeatability.
- **Use error bars** and statistical metrics (e.g., standard deviation, R^2 between simulation and experiment).
- Calibrate sensors rigorously and perform uncertainty propagation analysis.

Despite these caveats, the data support the conclusion that the machine fulfils its design purpose accurate tensile testing of SMA specimens at controlled thermal and mechanical conditions with a minimal cost.

4.0 Conclusion and Recommendations

This work successfully demonstrates the design and construction of a low-cost tensile testing machine capable of precise laboratory characterization of Shape Memory Alloys. The integration of electromechanical actuation, microcontroller-based control, and thermal regulation enables accurate evaluation of SMA mechanical and thermo-mechanical properties. Experimental validation using SMA springs showed close agreement between measured stress–strain curves and numerical simulations, confirming the accuracy and reliability of the system. The compact, modular design, combined with the use of readily available components, ensures affordability and ease of replication in academic and research laboratories, particularly in resource-limited environments. While the current design meets the essential requirements for SMA testing, future work will focus on expanding the load range, enhancing automation for real-time data acquisition, and extending testing capabilities to include other

SMA forms such as wires and thin films. The developed system provides a valuable platform for both research and educational purposes, bridging the gap between high-end commercial solutions and the need for accessible, functional laboratory equipment.

Declarations

Ethical Approval and Consent to Participate:

Informed consent, both verbal and written, was obtained from all participants before data collection. The study was conducted with full transparency.

Consent for Publication:

All authors consent to the publication of this manuscript and confirm that the work is original, has not been published elsewhere, and is not under consideration for publication elsewhere.

Competing Interests:

The authors declare no competing interests related to this study.

Funding:

This study did not receive any specific funding.

Data Availability:

The datasets generated and analyzed during the current study are available from the corresponding author upon reasonable request.

Authors' Contributions:

Abubakar Rabiu.A.: Conceptualization, methodology, and manuscript drafting. Abubakar Rabiu.A, Waqas Hafiz M: Data collection, analysis, and figure preparation. Abubakar Rabiu.A, Waqas Hafiz M, Gbaakpen Msughter: Literature review and critical manuscript revision. All authors read and approved the final manuscript.

Acknowledgment

The authors gratefully acknowledge the valuable contributions and support received during this study. We extend our sincere thanks to the mechanical engineering department for providing the necessary facilities and resources. Special appreciation is extended to our supervisor Prof. Linxiang Wang whose insights and feedback significantly improved the quality of this work. We also thank the anonymous reviewers for their constructive comments and suggestions which helped enhance the manuscript.

References

[1] M. P. Norton, *Introduction to Engineering Materials: Behavior, Properties, and Selection*, 2nd ed. New York, NY, USA: Prentice Hall, 2000.

[2] A. G. Guy, *Elements of Physical Metallurgy*, 3rd ed. Reading, MA, USA: Addison-Wesley, 1990.

[3] W. D. Callister and D. G. Rethwisch, *Materials Science and Engineering: An Introduction*, 9th ed. Hoboken, NJ, USA: Wiley, 2014.

[4] J. R. Davis, *Tensile Testing*, 2nd ed. Materials Park, OH, USA: ASM International, 2004.

[5] G. E. Dieter and D. Bacon, *Mechanical Metallurgy*, 3rd ed. London, U.K.: McGraw-Hill, 1986.

[6] L. Gardner, "Testing of materials in tension and compression," *Mater. Struct.*, vol. 41, no. 2, pp. 197–210, 2008, doi: 10.1617/s11527-007-9266-7.

[7] K. S. Lee and Y. J. Kim, "Development of a bench-top tensile testing machine for metallic materials," *J. Mech. Sci. Technol.*, vol. 30, no. 4, pp. 1603–1610, 2016, doi: 10.1007/s12206-016-0302-6.

[8] C. Pagliarulo and M. Maggiore, "An Arduino-based material testing machine," *IEEE Instrum. Meas. Mag.*, vol. 23, no. 6, pp. 34–39, 2020, doi: 10.1109/MIM.2020.9245636.

[9] A. Del Corso, L. M. Raffo, and G. S. Biglino, "Compact tensile tester for cyclic loading of superelastic biomaterials," *Biomed. Microdevices*, vol. 14, pp. 1039–1047, 2012, doi: 10.1007/s10544-012-9682-7.

[10] M. Kohl, *Shape Memory Microactuators*, Berlin, Germany: Springer, 2004, doi: 10.1007/978-3-540-40906-4.

[11] T. Duerig, K. Melton, D. Stöckel, and C. Wayman, *Engineering Aspects of Shape Memory Alloys*, London, U.K.: Butterworth-Heinemann, 1990, doi: 10.1016/B978-0-08-032603-0.50005-8.

[12] H. Tobushi, T. Hachisuka, and S. Ikai, "Low-cycle fatigue of a TiNi shape memory alloy and fracture mechanism," *JSME Int. J. Ser. I*, vol. 37, no. 3, pp. 433–440, 1994, doi: 10.1299/jsmeintl.37.433.

[13] Y. Zhang et al., "Design and development of a micro-tensile testing platform for characterizing SMA wires," *Sensors Actuators A Phys.*, vol. 249, pp. 8–14, 2016, doi: 10.1016/j.sna.2016.08.032.

[14] J. M. Dulieu-Barton et al., "Full-field strain measurements for characterizing the thermo-mechanical response of SMAs," *Exp. Mech.*, vol. 49, pp. 257–268, 2009, doi: 10.1007/s11340-008-9155-5.

[15] B. Shaw and S. Kyriakides, "Thermomechanical aspects of NiTi," *J. Mech. Phys. Solids*, vol. 43, pp. 1243–1281, 1995, doi: 10.1016/0022-5096(95)00017-8.

[16] C. Pagliarulo and M. Maggiore, "An Arduino-based material testing machine," *IEEE Instrum. Meas. Mag.*, vol. 23, no. 6, pp. 34–39, 2020, doi: 10.1109/MIM.2020.9245636.

[17] H. Liu and X. Yang, "Design of a low-cost tensile testing system with LabVIEW interface," *IOP Conf. Ser.: Mater. Sci. Eng.*, vol. 392, 032057, 2018, doi: 10.1088/1757-899X/392/3/032057.

[18] F. Auricchio et al., "A three-dimensional model describing stress-temperature induced solid phase transformation: Solution algorithm and boundary value problems," *Int. J. Numer. Methods Eng.*, vol. 62, pp. 415–449, 2005, doi: 10.1002/nme.1187.

[19] A. Khalil et al., "Development of a low-cost tensile testing machine with thermal regulation for SMA testing," *Mater. Today: Proc.*, vol. 47, no. 10, pp. 2663–2670, 2021, doi: 10.1016/j.matpr.2021.05.472.

[20] M. S. Mohd Jani, M. Leary, A. Subic, and M. A. Gibson, "A review of shape memory alloy research, applications, and opportunities," *Mater. Des.*, vol. 56, pp. 1078–1113, 2014, doi: 10.1016/j.matdes.2013.11.084.

[21] S. Miyazaki et al., "Mechanical properties of NiTi shape memory alloy wires: Size effects," *Mater. Sci. Eng. A*, vol. 438–440, pp. 18–22, 2006, doi: 10.1016/j.msea.2006.02.146.

[22] Y. Fu, W. Huang, H. Du, X. Huang, and J. Tan, "Design and fabrication of micro SMA tensile grips," *Microsyst. Technol.*, vol. 11, pp. 314–319, 2005, doi: 10.1007/s00542-004-0422-2.

[23] L. Heller and V. Harapiak, "Miniature extensometers for tensile testing of SMA wires," *Exp. Mech.*, vol. 52, no. 3, pp. 287–293, 2012, doi: 10.1007/s11340-011-9523-2.

[24] G. Udupa, S. Rao, and V. Dinesh, "Development of low-cost modular tensile testing machine for educational laboratories," *Procedia Eng.*, vol. 149, pp. 60–65, 2016, doi: 10.1016/j.proeng.2016.06.639.

[25] N. Ezeanya, C. Okoro, and A. Eboh, "Design and fabrication of a locally made tensile testing machine," *Niger. J. Technol.*, vol. 39, no. 2, pp. 345–350, 2020, doi: 10.4314/njt.v39i2.23.

[26] F. Veysset, K. Koenig, C. B. Roth, and K. A. Nelson, "A simple and inexpensive tensile tester for thin films of soft materials," *Rev. Sci. Instrum.*, vol. 89, no. 10, pp. 105108, 2018, doi: 10.1063/1.5042043.

[27] D. Solovei, M. Moldovan, and M. Grigore, "Low-cost tensile testing machine for soft materials used in engineering education," in *Proc. 2020 IEEE Global Engineering Education Conference (EDUCON)*, pp. 1628–1631, 2020, doi: 10.1109/EDUCON45650.2020.9125384.

